An optimisation method for the over-zero switching scheme

Flow Measurement and Instrumentation 27 (2012) 47–52

Contents lists available at SciVerse ScienceDirect

Flow Measurement and Instrumentation

journal homepage: www.elsevier.com/locate/flowmeasinst

An optimisation method for the over-zero switching scheme

Jiabin Jia *, Mi Wang

Institute of Particle Science and Engineering, School of Process, Environmental and Materials Engineering, University of Leeds, Leeds, LS2 9JT, UK

ARTICLE INFO

Keywords:
Over-zero switching scheme
Electrical impedance tomography
RC circuit

ABSTRACT

Due to the presence of a capacitive component on the Electrical Impedance Tomography (EIT)'s excitation and measurement interface, the Over-Zero Switching (OZS) scheme was proposed previously to eliminate the effect of transient time, increase the speed of data acquisition and improve the accuracy. The switching timing in relation to the sinusoidal excitation plays an important role in the OZS scheme. However, the correct setting of switching timing is normally based on trial-by-error, which has experienced a difficulty in the system set-up process. This paper presents an optimisation method for OZS based on the analysis of the electrical impedance of a sensor's interface. A simple equivalent RC circuit is utilised to simulate the sensor's excitation interface. By analysing the transient process of the RC circuit, the relationship between the optimal OZS timing and the phase angle of the equivalent impedance is established. In practice, the OZS timing and the impedance phase angle can be calculated from online measurements within a one quarter sinusoidal period. The experimental results show that the optimisation method is able to set the optimal OZS timing for a process medium with different electrical impedance property in EIT applications.

1. Introduction

In the operation of Electrical Impedance Tomography (EIT), the excitation source of EIT is frequently switched to different electrodes. Due to the presence of capacitive components in the electrode–electrolyte interface and a medium, the signal transient time of the sensor (the electrode–electrolyte interface in the case of EIT) is normally not negligible, which will limit the data acquisition speed and may affect the measurement accuracy. This problem has been reviewed previously [1]. By analysing the equivalent circuit of the electrode–electrolyte interface and an AC coupling circuit, the genuine restriction of EIT speed was investigated and the Over-Zero Switching (OZS) scheme was proposed to eliminate the transient time effect for an EIT system with current excitation sources. The EIT system with the OZS scheme achieved the data acquisition speed more than 1000 dual-frames per second [2,3]. However, to date, there is no practical way to determine online the optimal OZS timing for applications with different mediums. The different switching timing has to be attempted repetitively until the best measurement profile appears, which is time-consuming, less effective and undesirable in operation. Moreover, since the process medium inside the process vessels or pipes may change all the time, the previously established OZS switching timing may not fit the late situations. A more intelligent approach is needed to automatically obtain the optimal OZS timing corresponding to the change of the process medium in the process.

2. Over-zero switching for EIT with a voltage-source

2.1. Simplified EIT model

The proposed method is limited to flows having a conductive continuous phase. The material of the electrodes and the physicochemical property of the medium in the process will influence the equivalent impedance of the EIT sensor's interface, because the conductivity or ionic concentration of the conductive continuous phase of flows directly affects the value of the capacitive components of the electrode–electrolyte interface [4]. In this study, the four-terminal EIT electrical model [5] for a high frequency sinusoidal excitation (>1 kHz) is further simplified to an equivalent circuit just consisting of an equivalent resistor R and an equivalent capacitor C in series, as shown in Fig. 1, where R denotes the bulk resistance and all other resistance in the sensing interface and C denotes the double layer capacitance at the electrode–electrolyte and all other capacitance in the sensing interface. Both R and C vary in a particular process medium; however, the change of process medium cannot be completely finished within a short period of time. When the single-pole double throw switch S is in position 1, the capacitor C is charged. The residual potential across the capacitor C charged from the previous operation is released when the switch is moved to position 2. The timing of switching operations between positions 1 and 2 crucially affects the transmit process [6].

* Corresponding author. Tel.: +44 1133432357.
E-mail address: prejj@leeds.ac.uk (J. Jia).

0955-5986/$ – see front matter © 2012 Elsevier Ltd. All rights reserved.
doi:10.1016/j.flowmeasinst.2012.02.002

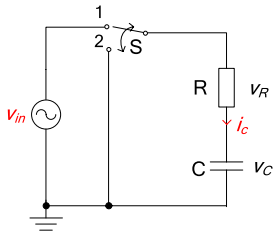

Fig. 1. Simplified equivalent circuit of EIT medium.

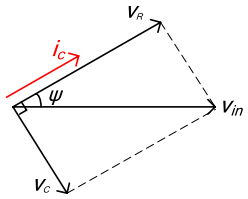

Fig. 2. Vector diagram of an *RC* circuit in series.

2.2. Over-zero switch for EIT with voltage source

It is well known that a capacitor naturally resists the voltage change across it and therefore, a transient time usually presents when a capacitor is used for an alternating current (AC) signal coupling. However, if the residual voltage remaining on the capacitor is the same as the applied voltage in the switching operation, no transient process occurs. For example, when both the instantaneously applied voltage v_C and the residual voltage across the capacitor C are equal to zero, no charging or discharging process happens when the switch S is thrown to position 1, which is how the term, over-zero switching comes up.

In Fig. 1, the equivalent load impedance consisting of the resistor R and capacitor C in series is expressed as Z:

$$Z = R - j\frac{1}{\omega C}. \tag{1}$$

The phase angle of equivalent load impedance, ψ, is denoted as Eq. (2):

$$\psi = \tan^{-1}\left(-\frac{1}{RC\omega}\right). \tag{2}$$

The vector diagram of the RC circuit (Fig. 2) interprets that the current, i_C, is ahead of the applied voltage, v_{in}, with a phase angle ψ. This angle ψ might vary from 0° to 90° when the values of R and C change. According to the nature of the capacitor, the voltage, v_C, across the capacitor C lags the current i_C 90°. In other words, the current i_C through the capacitor reaches its peak value; simultaneously, the voltage v_C, across the capacitor is exactly zero.

The relationship between the voltage v_C and the current i_C is denoted as:

$$i_C(t) = C\frac{dv_C}{dt}. \tag{3}$$

Based on Fig. 1, the AC voltage excitation source $v_{in}(t)$ can be expressed as Eq. (4).

$$v_{in}(t) = V\sin(\omega t) = \left(R - j\frac{1}{\omega C}\right) i_C(t). \tag{4}$$

The former two equations are combined as:

$$v_{in}(t) = \left(R - j\frac{1}{\omega C}\right) C\frac{dv_C}{dt}. \tag{5}$$

After Laplace transformation on both sides of Eqs. (4) and (5), they are transformed into Eqs. (6) and (7), respectively.

$$V_{in}(s) = \frac{V\omega}{s^2+\omega^2} \tag{6}$$

$$\left(R + \frac{1}{Cs}\right) C[sV_C(s) - V_C(0^-)] = \frac{V\omega}{s^2+\omega^2} \tag{7}$$

where $V_C(0^-)$ is the initial voltage across the capacitor C before switch S is thrown to position 1 (Fig. 1). Rearranging and decomposing Eq. (7) gives Eq. (8).

$$\begin{aligned} V_C(s) &= \frac{V\omega}{(1+RCs)(s^2+\omega^2)} + \frac{V_C(0^-)}{s} \\ &= \frac{\frac{V\tau\omega s}{1+\tau^2\omega^2}}{s^2+\omega^2} + \frac{\frac{V\omega}{1+\tau^2\omega^2}}{s^2+\omega^2} + \frac{\frac{V\tau^2\omega}{1+\tau^2\omega^2}}{\tau s+1} + \frac{V_C(0^-)}{s} \end{aligned} \tag{8}$$

where the time constant, τ, equals RC.

The inverse Laplace transformation of Eq. (8) is conducted to get Eq. (9), base on the assumptions of Eqs. (10)–(12):

$$\begin{aligned} v_C(t) &= -\frac{V\tau\omega}{1+\tau^2\omega^2}\cos(\omega t) + \frac{V}{1+\tau^2\omega^2}\sin(\omega t) \\ &\quad + \frac{V\tau\omega}{1+\tau^2\omega^2}e^{-t/\tau} + V_C(0^-) \\ &= \frac{V}{\sqrt{1+\tau^2\omega^2}}\sin(\omega t+\theta) + \frac{V\tau\omega}{1+\tau^2\omega^2}e^{-t/\tau} + V_C(0^-) \end{aligned} \tag{9}$$

$$\sin(\theta) = -\frac{\tau\omega}{\sqrt{1+\tau^2\omega^2}} \tag{10}$$

$$\cos(\theta) = \frac{1}{\sqrt{1+\tau^2\omega^2}} \tag{11}$$

$$\theta = \tan^{-1}(-\tau\omega) = \tan^{-1}(-RC\omega). \tag{12}$$

The first term of Eq. (9) indicates that the sinusoidal response has the same frequency with the excitation source V_{in} and a phase shift θ. The second term represents the settling process of the transient response. The third term $V_C(0^-)$ is the residual potential across the capacitor C just before the switch S is thrown to the position 1 (Fig. 1). In other words, $V_C(0^-)$ directly relates to the previous operation. The residual potential across the capacitor C is the sum of all three terms of Eq. (9) whilst the switch S is moved from the position 1 to the position 2. If the sum of the first and second terms is zero, the initial voltage $V_C(0^-)$ for the next cycle is also zero and no transient time reacts.

An additional phase shift φ is introduced to control the switching position; then Eq. (4) is replaced by Eq. (13).

$$v_{in}(t) = V\sin(\omega t+\varphi). \tag{13}$$

Correspondingly, Eq. (9) is deduced as Eq. (14),

$$\begin{aligned} v_C(t) &= \frac{V}{\sqrt{1+\tau^2\omega^2}}\sin(\omega t+\theta+\varphi) \\ &\quad + \frac{V\tau\omega}{\sqrt{1+\tau^2\omega^2}}e^{-t/\tau}\sin(\theta+\varphi) + V_C(0^-). \end{aligned} \tag{14}$$

In order to make $v_C(t)$ equal to zero whilst the switch S is thrown to the position 1 ($t = 0$), the first two terms have to be zero. Therefore, Eqs. (15) and (16) have to be satisfied at the same time:

$$\omega_t + \theta + \varphi = n\pi \quad (n = 0, 1, 2, 3, \ldots) \tag{15}$$

$$\theta + \varphi = m\pi \quad (m = 0, 1, 2, 3, \ldots). \tag{16}$$

When $n = m = 0$, then

$$\varphi = -\theta. \tag{17}$$

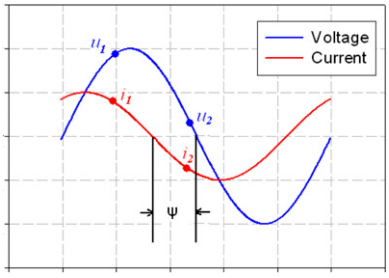

Fig. 3. Two point sampling method for the impedance phase calculation.

According to the trigonometric formula given below (if $x < 0$):

$$\tan^{-1}(x) = -\frac{\pi}{2} - \tan^{-1}\left(\frac{1}{x}\right). \tag{18}$$

Eq. (12) is transformed into

$$\theta = \tan^{-1}(-RC\omega) = -\frac{\pi}{2} - \tan^{-1}\left(-\frac{1}{RC\omega}\right). \tag{19}$$

Combining Eqs. (17) and (19), the phase shift φ is derived by the equation below:

$$\varphi = -\theta = \frac{\pi}{2} + \tan^{-1}\left(-\frac{1}{RC\omega}\right). \tag{20}$$

Combining Eqs. (2) and (20), Eq. (21) is obtained. If the real-time phase angle, ψ, of equivalent load impedance can be determined quickly, the additional phase shift φ can be implemented to eliminate transient time, which is referred as OZS angle.

$$\varphi = \frac{\pi}{2} + \Psi. \tag{21}$$

An algorithm is introduced below to calculate the real-time ψ of the variable load (medium).

2.3. Quarter sampling algorithm

Since the applied voltage and current are measured at the same time by the EIT system with a voltage excitation source [7], the calculations of the real-time phase angle of the equivalent impedance become possible. In contrast, the traditional EIT systems only sample the voltage signals but the current is assumed as a known constant.

In the schematic diagram Fig. 3, two voltages u_1 and u_2 with a 90° phase difference are sampled and two currents i_1 and i_2 are synchronically sampled as well. The ψ is the phase angle displacement between the current and voltage.

It is assumed that the amplitudes of the voltage current signals U_m and I_m are constant over a short period of time. The values of the four sampled points are described by the following equations.

$$u_1 = U_m \sin(\omega t + \varphi) \tag{22}$$

$$u_2 = U_m \sin\left(\omega t + \varphi + \frac{\pi}{2}\right) \tag{23}$$

$$i_1 = I_m \sin(\omega t + \varphi + \Psi) \tag{24}$$

$$i_2 = I_m \sin\left(\omega t + \varphi + \frac{\pi}{2} + \Psi\right). \tag{25}$$

Mutually multiplying u_1, u_2, i_1 and i_2 and summing the products:

$$\begin{aligned} u_1 i_2 - u_2 i_1 &= -\frac{1}{2}U_m I_m\left[\cos\left(2\omega t + 2\varphi + \frac{\pi}{2} + \psi\right) + \sin(\psi)\right] \\ &\quad + \frac{1}{2}U_m I_m\left[\cos\left(2\omega t + 2\varphi + \frac{\pi}{2} + \psi\right) - \sin(\psi)\right] \\ &= -U_m I_m \sin(\psi) \end{aligned} \tag{26}$$

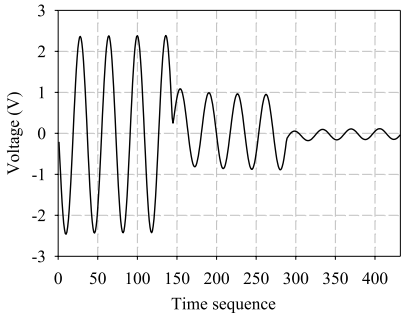

Fig. 4. Recorded signal waveform on a pair of electrodes without OZS timing control.

$$\begin{aligned} u_1 i_1 + u_2 i_2 &= -\frac{1}{2}U_m I_m[\cos(2\omega t + 2\varphi - \psi) - \cos(\psi)] \\ &\quad - \frac{1}{2}U_m I_m\left[\cos\left(2\omega t + 2\varphi + \pi + \psi\right) - \cos(\psi)\right] \\ &= U_m I_m \cos(\psi). \end{aligned} \tag{27}$$

The phase angle ψ of an equivalent load impedance in Fig. 1 can be derived from the ratio of Eqs. (26) and (27).

$$-\frac{u_1 i_2 - u_2 i_1}{u_1 i_1 + u_2 i_2} = \tan(\Psi) \tag{28}$$

$$\Psi = \tan^{-1}\left(-\frac{u_1 i_2 - u_2 i_1}{u_1 i_1 + u_2 i_2}\right). \tag{29}$$

The advantage of this algorithm is that it only takes a quarter period to get the real-time phase information of impedance.

2.4. Experimental verification

To verify the effectiveness of the optimisation method for controlling OZS timing, a series of experiments from a water phantom were carried out. A cylindrical Perspex vessel was used. Its internal diameter was 0.148 m and the height of the interior solution remained 0.06 m. Sixteen electrodes made from stainless-steel with the dimension 0.01 m × 0.03 m × 0.005 m (length × width × thickness) were equally spaced on the inner wall of the vessel to form a one plane EIT sensor. The frequency of excitation single is 10 kHz. The conductivity of sodium chloride solution was maintained as 0.351 S/m, 1.450 S/m and 2.330 S/m, with respect to each test. The phase angles of equivalent load impedances, ψ, in regard to different solutions, were calculated by the use of the quarter sampling algorithm. Then, the OZS angles, φ, for these set-ups were derived from the relationship of Eq. (21). The consequences of applying the OZS angle to the switching timing are compared with those of applications without the OZS angle. In practice, the switching operation was implemented by controlling the delay time between the excitation signal and the switching pulse.

When the conductivity of the solution was 0.351 S/m and no OZS angle was applied, for simplicity, only a part of the continuous signal on the same pair of adjacent electrodes was recorded and shown in Fig. 4. The transient process can be easily observed in this part. The changes of amplitude in Fig. 4 are due to the roles of electrodes changing between excitation and measurement. During the first 4 periods, the electrode pair worked as an excitation source. Afterwards, this pair acted as responding electrodes because the excitation source was switched to its adjacent pair of electrodes. A minor transient process occurs due to the mismatch of switching, which can only be found from the initial stage of the waveform in Fig. 4, although they are hard to notice in the typical EIT voltage profile in Fig. 5, which is derived from Fig. 4. The voltage profile composed of 104 independent measurement

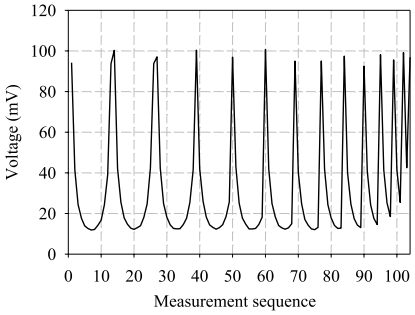

Fig. 5. Voltage profile of conductivity 0.351 S/m without OZS timing control.

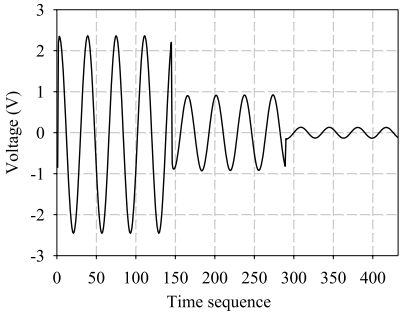

Fig. 6. Recorded signal waveform on a pair of electrodes with OZS timing control.

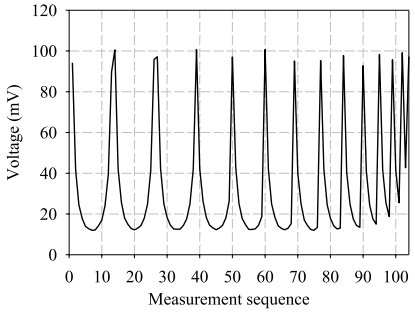

Fig. 7. Voltage profile of conductivity 0.351 S/m with OZS timing control.

points in Fig. 5 nearly shows a standard and smooth U-shaped voltage measurement set of EIT.

The phase angle of equivalent load impedance 12.02° was calculated with the quarter sampling algorithm in terms of Eq. (29). 102.02° OZS angle from Eq. (21) was applied to the switching control. The same measurement was taken and a part of response voltage on the pair of adjacent electrodes and the voltage profile was recorded in Figs. 6 and 7. Compared with Fig. 4, the transient process in Fig. 6 is almost eliminated. However, voltage profiles in Figs. 5 and 7 have no apparent difference, because the conductivity of the solution is relatively low and capacitive reactance has a small proportion among total impedance, transient time does not have a great effect (referring to the *RC* model given in Fig. 1), even without the application of the over-zero switching control.

Fig. 8 displays the switching signal and the voltage and the enlarged current waveform of the voltage source output, which were captured from an oscilloscope. According to the analysis in Section 2.2, the switching point takes place on the peak of the current waveform whilst the voltage across the equivalent capacitor *C* in Fig. 1 is zero.

When the conductivity of the solution was increased to 1.450 S/m and no OZS angle was applied, a part of the continuous signal

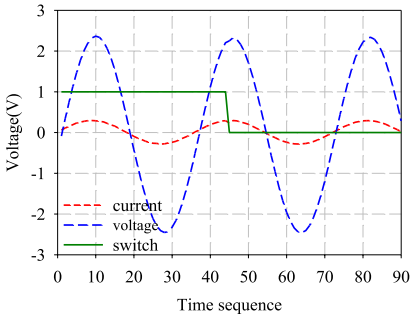

Fig. 8. Relative phase of voltage, current and switching signal.

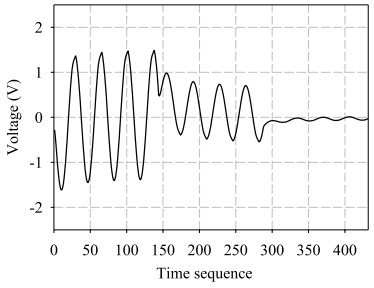

Fig. 9. Recorded signal waveform on a pair of electrodes without OZS timing control.

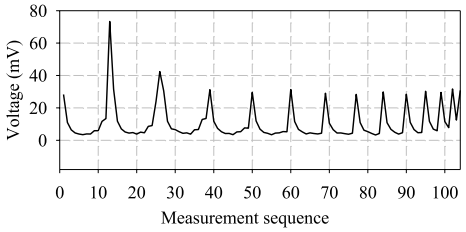

Fig. 10. Voltage profile of conductivity 1.450 S/m without OZS timing control.

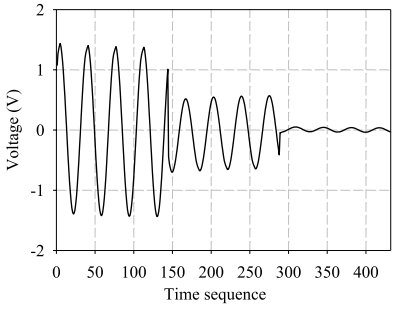

Fig. 11. Recorded signal waveform on a pair of electrodes with OZS timing control.

on the same pair of adjacent electrodes was recorded again and shown in Fig. 9. A clear transient process presents after switching operations; therefore, the voltage profile displayed in Fig. 10 is not as smooth as Fig. 5, particularly at lower areas of the profile. To avoid the disturbance of the transient process, the conventional method is that the sampled data from the first few periods must be abandoned, which causes a prolonging process and a slower systematic speed.

In this case, the phase angle of equivalent load impedances, ψ, 23.48° was obtained and the OZS angle 113.48° was applied; compared with Fig. 9, the transient process is significantly removed

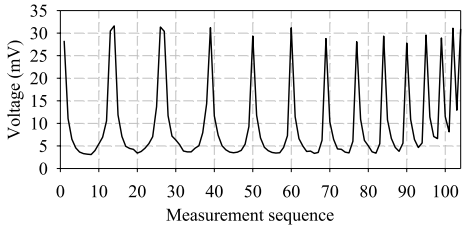

Fig. 12. Voltage profile of conductivity 1.450 S/m with OZS timing control.

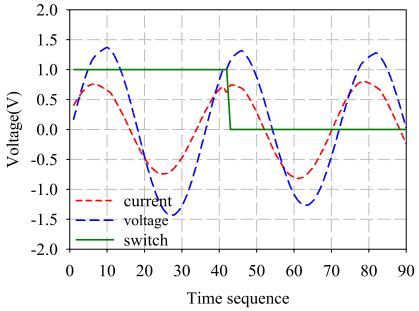

Fig. 13. Relative phase of voltage, current and switching signal.

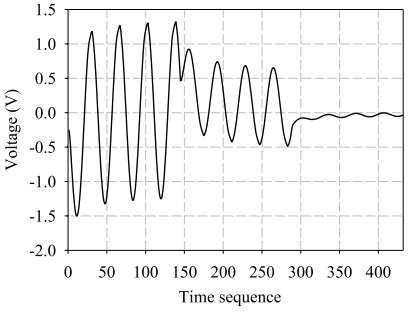

Fig. 14. Recorded signal waveform on a pair of electrodes without OZS timing control.

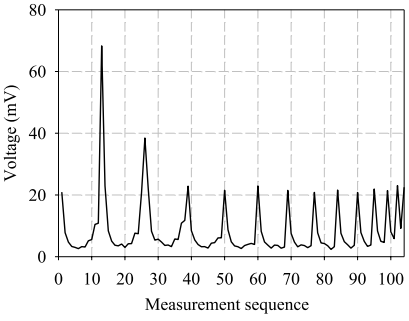

Fig. 15. Voltage profile of conductivity 2.330 S/m without OZS timing control.

in Fig. 11. The voltage profile in Fig. 12 nearly becomes standard shape.

Fig. 13 illustrates the voltage and current waveforms from the voltage source output. The switching control takes place on the peak of the current waveform again.

When the conductivity of the solution was increased to 2.330 S/m and no phase shift was applied, a part of the continuous signal on the pair of adjacent electrodes was recorded and shown in Fig. 14. The severe transient process exhibits after the switching operations take place. The corresponding voltage profile in Fig. 15 has the abnormal shape.

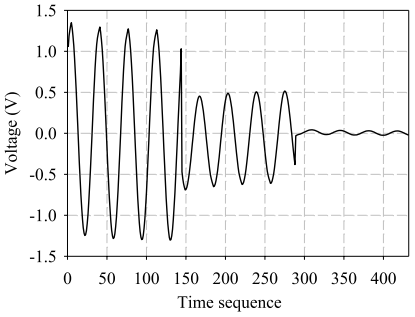

Fig. 16. Recorded signal waveform on a pair of electrodes with OZS timing control.

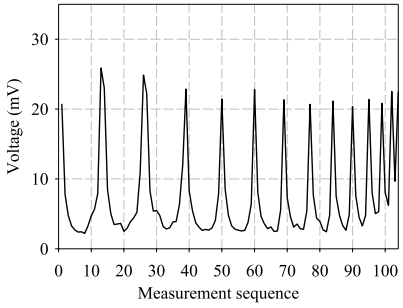

Fig. 17. Voltage profile of conductivity 2.330 S/m with OZS timing control.

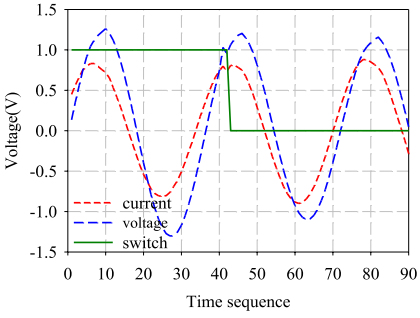

Fig. 18. Relative phase of voltage, current and switching signal.

The phase angle 25.41° was calculated and phase shift 115.41° was applied. Compared with Fig. 14, the transient process is considerably reduced in Fig. 16. Minor overadjustments appear in Figs. 11 and 16; it might be due to approximation in the electrical model and the inaccuracy of the sampled signal. The voltage profile in Fig. 17 is much better than that of Fig. 15.

Fig. 18 illustrates the voltage and current waveform of the voltage source and switching signal. The switching point is located on the peak of current, which proves the principle of switching optimisation inferred in Section 2.2 again.

The experimental results above demonstrate without the phase shift control, the long transient time exists and affects the shape of the voltage profile. The quarter sampling algorithm detects the specific phase angle for different equivalent impedance. Then, the optimal over-zero switching shift can effectively reduce the transient time.

To quantitatively evaluate the benefit of the proposed method, another experiment was conducted. Without OZS application, 100 periods (10 ms) of excitation rather than 4 periods were maintained to let the circuit fully reach its steady state after each switching. The process from transient state to steady state is displayed in Fig. 19. The phase angle calculated from the current and voltage samples is 25.70° and the impedance is

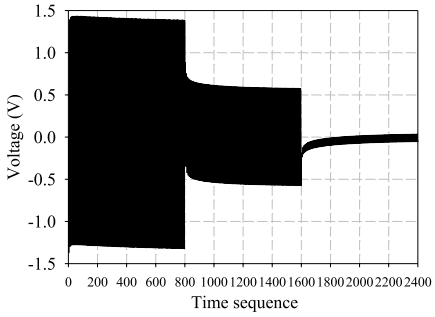

Fig. 19. Transient state to steady state without OZS timing control.

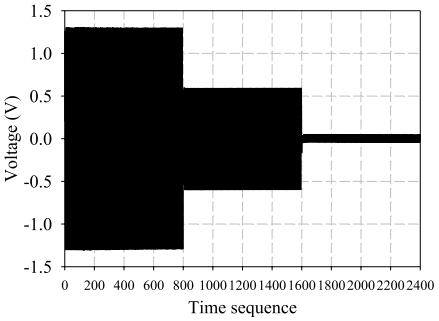

Fig. 20. Absence of transient state with OZS control.

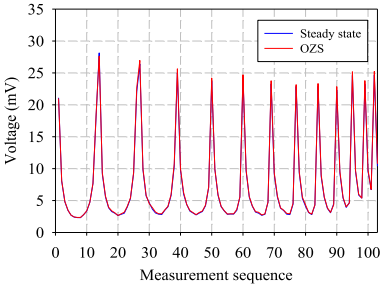

Fig. 21. Comparison of voltage profiles from steady state and OZS. (For interpretation of the references to colour in this figure legend, the reader is referred to the web version of this article.)

2.51 Ω. Therefore, the resistance R and the reactance X are 2.26 Ω and 1.09 Ω, respectively. At the frequency 10 kHz, the capacitance associated with reactance is 14.60 μF. Time constant RC is 33.00 μs. As shown in Fig. 19, after 4.95 ms (150 times of time constant), the steady state presents that, if without OZS application, this time delay has to wait before data acquisition. The experiment was repeated with OZS application, as shown in Fig. 20, the transient process is avoided.

Without OZS application, when the circuit reaches the steady state, the voltage profile V_1 (blue curve in Fig. 21) is extracted from Fig. 19 and plotted. With OZS application, the voltage profile V_2 (red curve in Fig. 21) is extracted from Fig. 20 and plotted again. Two curves look nearly overlapped. The relative difference between V_1 and V_2 is plotted in Fig. 22. The root-mean square of relative difference (RMS_{rd}) is defined by Eq. (30). RMS_{rd} value in Fig. 22 is only 2.45%. This experiment demonstrates that it is not

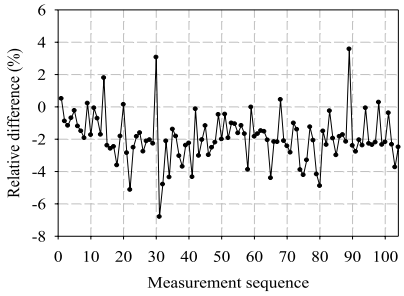

Fig. 22. Relative difference between two voltage profiles.

necessary to wait till the circuit reaches its steady state anymore if the optimised OZS is applied.

$$RMS_{rc} = 100\% \times \sqrt{\frac{1}{104}\sum_{i=1}^{104}\left(\frac{V_{1_i} - V_{2_i}}{V_{1_i}}\right)^2}. \tag{30}$$

3. Conclusions

Because of the capacitive component in the sensor's interfaces, typically the electrode–electrolyte interfaces of electrical impedance tomography, the transient time of the sensing signal in frequently switching operations of a sensor's excitation and measurement may affect the measurement accuracy and therefore limit the data acquisition speed. An optimisation method from further analysis of the OZS scheme is proposed in the paper by theoretically deducing the relationship between the OZS angle (timing) and the impedance phase angle with a simplified RC equivalent circuit. A quarter sampling algorithm has also been proposed to obtain the impedance phase angle by simultaneously sampling the voltage output and current output of the voltage excitation source in only a quarter period of the signal. Therefore, the optimal OZS timing could be online-deduced to meet the dynamic change of the process medium's conditions. The experiments by varying the medium conductivity over a wide range demonstrate the excellent capability of the proposed method for overcoming the effects of signal transient time.

References

[1] Wang M, Ma Y. Over-zero switching scheme for fast data collection operation in electrical impedance tomography. Measurement Science & Technology 2006; 17:2078–82.
[2] Schlaberg HI, Jia J, Qiu C, Wang M, Li H. Development and application of the fast impedance camera — a high performance dual-plane electrical impedance tomography system. In: 5th international symposium on process tomography. Poland (Zakopane); 2008.
[3] Xu C, Zhang ZQ, Han J, Dong F. A parallel data acquisition system based on CPCI for ERT. In: Proceedings of 6th world congress on industrial process tomography. Beijing; 2010.
[4] Wang M. Electrode models in electrical impedance tomography. Journal of Zhejiang University SCIENCE 2005.
[5] Szczepanik Z, Rucki Z. Frequency analysis of electrical impedance tomography system. IEEE Transactions on Instrumentation and Measurement 2000;49: 844–51.
[6] Ma Y, Lai Y, Wang M, Jia J. Experimental validation of over-zero switching method. In: What, where, when: multi-dimensional advances for industrial process monitoring international symposium (W3MDM). Leeds (UK); 2009.
[7] Jia J, Wang M, Schlaberg HI, Li H. A novel tomographic sensing system for high electrically conductive multiphase flow measurement. Flow Measurement and Instrumentation 2010;21:184–90.